The Regulation of Insulin Receptor/insulin-like Growth Factor Receptor Ratio, an Important Factor for Breast Cancer Prognosis, by TRIP-Br1

Nguyen Thi Ngoc Quynh
Sookmyung Women's University
Samil Jung
Sookmyung Women's University
Nguyen Hai Anh
Sookmyung Women's University
Beom Suk Lee
Sookmyung Women's University
Davaajargal Myagmarjav
Sookmyung Women's University
Hye Hyeon Eum
The Catholic University of Korea
Hae-Ock Lee
The Catholic University of Korea
Taeyeon Jo
Sookmyung Women's University
Raj Kumar Mongre
University of Rochester Medical Center
Yeongseon Choi
Sookmyung Women's University
Myeong-Sok Lee (mslee@sookmyung.ac.kr)
Sookmyung Women's University

Research Article

Keywords: breast cancer, IR, IGF1R, TRIP-Br1, NEDD4-1

Posted Date: March 15th, 2022

DOI: https://doi.org/10.21203/rs.3.rs-1429530/v1

Abstract

Much higher risk of cancer is observed in patients with diabetes. Insulin receptor (IR) and insulin-like growth factor-1 receptor (IGF1R) are well-known targets in cancer research as well as diabetes treatment. Interestingly, a recent study proposed that the IR/IGF1R ratio is an important factor in breast cancer prognosis. Women with a higher IR/IGF1R ratio showed poor breast cancer prognosis and hyperinsulinemia. Here, we propose a novel mechanism by which the oncogenic protein TRIP-Br1 renders breast cancer cells to have a higher IR/IGF1R ratio by positively and negatively regulating IR and IGF1R expression at the protein level, respectively. TRIP-Br1 plays various cellular roles, one of which is as an adaptor protein. Our data revealed that TRIP-Br1 suppresses ubiquitin/proteasome-mediated IR degradation without directly interacting with IR. Meanwhile, TRIP-Br1 directly interacts with both IGF1R and NEDD4-1 E3 ubiquitin ligase, and TRIP-Br1/NEDD4-1 degrades IGF1R via the ubiquitin/proteasome system. Animal experiments indicated that TRIP-Br1 enhanced tumor progression, where a high IR/IGF1R ratio was detected. Furthermore, IR silencing elevates IGF1R expression, resulting in a lower IR/IGF1R ratio. Our extended study showed a similar effect of TRIP-Br1 on the IR/IGF1R ratio in insulin-deficient mice mimicking patients with diabetes, confirming the strong relationship between breast cancer and diabetes. In conclusion, this study provides invaluable information on the regulatory mechanism of how breast cancer cells acquire a higher IR/IGF1R ratio.

Introduction

According to the World Health Organization (WHO), cancer remains a major threat to human health, and is currently the second most common cause of death [1]. Breast cancer is the most common type of cancer in women, with 19.3 million cases and 10 million cancer-related deaths reported in 2020 [2]. Thus, there is an urgent need to identify potential targets involved in breast cancer to aid in the development of efficient therapies. The relationship between breast cancer and diabetes has been extensively studied [3–8]. Women with diabetes are at a greater risk of developing breast cancer than those without diabetes [8–9]. This study attempts to understand the molecular mechanisms involved in both breast cancer and diabetes.

IR and IGF1R are the common targets in breast cancer and diabetes therapies. They share very high sequence homology and functional structures, such as the intracellular kinase domain [10–11]. In normal cells, both IR and IGF1R are activated by insulin and IGF1, which are well-known growth and survival factors. Insulin and IGF1 bind to IR and IGF1R in the form of homodimers or heterodimers with a very high affinity [12–14]. The binding of insulin and IGF1 to both receptors activates intrinsic receptor tyrosine kinase and downstream signaling cascades, which in turn regulate many cellular functions, including gene transcription, nutrient metabolism (glucose, lipids, and proteins), and cell growth and differentiation [15–17]. However, the aberrant expression and activation of IR and IGF1R are strongly associated with a greater risk of breast cancer [18–19]. IR and IGF1R are overexpressed in most cancer cells, including breast cancer cells [20–21]. Upregulated IR and IGF1R expression exacerbates tumorigenesis in cancer cells by activating many signaling pathways, including the phosphatidylinositol

3-kinase (PI3K)/protein kinase B (AKT) and mitogen-activated protein kinase (MAPK) pathways. IR- and IGF1R-mediated signaling pathways are highly activated in more than 75% of breast cancer patients and 87% of invasive breast cancer patients [22]. High levels of IR and IGF1R signaling pathway activation is closely associated with mammary tumor growth and proliferation, angiogenesis, immune suppression, metastasis, invasion, and suppressed apoptosis, which can result in the development of aggressive breast cancer [23–26]. Therefore, IR and IGF1R have received considerable attention as prominent targets for cancer prevention and therapy [27–28]. However, many cancer treatment studies have focused on targeting the expression and activation of either IR or IGF1R without considering the effects of both IR and IGF1R. An approach that co-targets both receptors may enhance the antitumor efficacy of the treatment of cancers.

It has been suggested that the inhibition of IGF1R alone does not affect tumor growth in preclinical trials, but enhances the IR signaling pathway [29]. IR has also been reported to enhance multistage tumor progression and convey intrinsic resistance to IGF1R targeted therapy, as an essential part of the tumor-promoting IGF signaling pathway [30]. Interestingly, a recent study suggested that the IR/IGF1R ratio is a key factor in breast cancer prognosis [31]. Gallagher *et al.* evaluated the IR/IGF1R ratio in over 500 patients with breast cancer [31]. They showed that breast cancer patients with a higher IR/IGF1R ratio due to elevated IR expression not only have hyperinsulinemia but are also more susceptible to tumorigenesis-promoting effects due to a greater sensitivity to the growth-promoting effects of insulin [31]. In an attempt to determine how the IR/IGF1R ratio can be regulated in breast cancer cells, we initially focused on the TRIP-Br1 oncogenic protein.

Previously, we showed that a deficiency of insulin or IGF1 greatly increased TRIP-Br1 gene expression in breast cancer cells. However, this expression was decreased to basal levels after the addition of insulin or IGF1, implying that TRIP-Br1 might be associated with insulin and IGF1-related signaling pathways [32]. Our own research and other groups have shown that TRIP-Br1 is significantly overexpressed in various cancers [33]. We also found that TRIP-Br1 expression greatly increased in various cancer cell lines, especially in breast cancer cell lines, compared to other types of cancer cell lines, in response to cell death-inducing stressful conditions (e.g., nutrient starvation and anticancer treatment) [33]. Upregulated TRIP-Br1 suppresses programmed cell death, such as apoptosis and necroptosis, in breast cancer cells as an oncoprotein [34]. TRIP-Br1 is known to be involved in various biological functions, including transcription, cell cycle progression, metabolism, programmed cell death, metastasis, invasion, and tumorigenesis [34–36]. TRIP-Br1 contains multiple protein-interacting domains, including an N-terminal putative cyclin-A-binding domain, a novel highly conserved SERTA domain, a binding motif for PHD zinc finger- and/or bromodomain-containing proteins, and an acidic C-terminal domain. These various protein-interacting domains seem to enable TRIP-Br1 to act as an adaptor protein [34, 37]. For example, TRIP-Br1 directly binds to two E3 ubiquitin ligases (NEDD4-1 and XIAP) and their target proteins (PTEN and adenylyl cyclase) as an adaptor protein, in which TRIP-Br1/E3 ligases induce the ubiquitination and degradation or cellular translocation of the target proteins [33, 37–40].

In this study, the regulatory mechanism of TRIP-Br1 in controlling the IR/IGF1R ratio in breast cancer cells is explored.

Materials And Methods

Cell lines and reagents. Cell lines were obtained from ATCC. Human MCF10A normal mammary epithelial cells were cultured as previously described [32]. Breast cancer cell lines and mouse embryonic fibroblast (MEF) cells were cultured in Dulbecco's modified Eagle's medium (DMEM) (Cat#31966–021; Life Technologies) supplemented with 10% fetal bovine serum (FBS) (Gibco) and a 1% antibiotic-antimycotic solution (Cat#15240-06, Gibco). All the cells were maintained at 37°C in a humidified atmosphere with 95% air and 5% CO_2. The reagents were purchased from the following manufacturers: MG132 (Cat#M-1157; A.G. Scientific Inc.), chloroquine (CQ) (Cat#C6628; Sigma-Aldrich), cycloheximide (CHX) (Cat#C7698; Sigma), and OSI-906 (Cat#S1091; Selleckchem).

Suppression or overexpression of TRIP-Br1, NEDD4-1, and IR. To repress TRIP-Br1 expression, cells were transfected with TRIP-Br1 silencing siRNA (siTRIP-Br1) (Cat#sc-62988; Santa Cruz Biotechnology) using Lipofectamine 2000 (Cat#11668; Invitrogen) in Opti-MEM (Cat#31985; Invitrogen), in which scrambled small interfering RNA (scRNA) was used as a control. $MCF7^{WT-TRIP-Br1}$ and $MCF7^{KD-TRIP-Br1}$ stable cell lines were established as described in our previous study [33]. To establish TRIP-Br1 overexpressing cells, cells were transfected with TRIP-Br1 overexpressing plasmid (pcDNA3.1/TRIP-Br1) using Lipofectamine 2000 in Opti-MEM medium. NEDD4-1 and IR genes were silenced using TurboFect Transfection Reagent (Cat #R0531; Thermo Scientific) with NEDD4-1 silencing siRNA (siNEDD4-1) or IR silencing RNA (siIR) from BIONEER Corporation (Korea) as follows:

siNEDD4-1: UUCCAUGAAUCUAGAAGAACATT/UGUUCUUCUAGAUUCAUGGAATT

siIR: GCAGGUCCCUUGGCGAUGU/ACAAGACCUAAGUGCACUG = tt

Cell viability analysis. Cell viability was analyzed using the Cell Viability, Proliferation & Cytotoxicity Assay Kit (Cat#EZ-3000; EZ-CYTOX) in accordance with the manufacturer's instructions by measuring the absorbance at 450 nm using a Gemini XPA Microplate Reader.

Western blot analysis. Western blot analysis of cell lines was performed as previously described [32]. For the western blot analysis of mouse tissue samples, tissues from mice were dissected, washed with PBS, and homogenized in RIPA buffer (50 mM Tris-HCl, 150 mM NaCl, 0.1% SDS, 0.5% sodium deoxycholate, 1% TritonX-100, 1 mM DTT, 1 mM PMSF, pH 7.4) supplemented with a protease inhibitor cocktail (Cat#P-1512; A.G. Scientific Inc.). After sonication, the tissue lysates were centrifuged at 16,000 · *g* for 20 min, and the supernatants were used for western blotting. The following antibodies were used: TRIP-Br1 (Cat #ALX – 804 – 645; Enzo Life Sciences), IR (Cat#57982; Cell Signaling), IGF1R (Cat#sc-81464; Santa Cruz Biotechnology, or Cat#ab39675; Abcam), IGF1R/IR (Cat#ab172965; Abcam), NEDD4-1 (Cat#sc-25508; Santa Cruz Biotechnology), insulin (Cat#ab63820; Abcam), glucagon (Cat#ab92517; Abcam), and β-actin (Cat#sc-47778; Santa Cruz Biotechnology).

Immunoprecipitation (IP). Cells were lysed in NP-40 lysis buffer (Cat #BA1049; Elpis Biotech) supplemented with a protease inhibitor cocktail for 20 min at 4°C. The lysate was centrifuged and the supernatant was incubated with the respective antibodies at 4°C overnight on a Rotospin (SLRM-2M; Mylab Intelli Mixer), followed by incubation with Protein G- or A-agarose beads (Cat#sc-2003; Santa Cruz Biotechnology) for 4 h at 4°C. The samples were then centrifuged and washed with NP40 lysis buffer. The proteins were eluted from the washed beads by boiling for 5 min in 4× SDS gel loading dye and were subjected to immunoblot analysis. Normal mouse IgG (Cat#sc-2025; Santa Cruz Biotechnology) and normal rabbit IgG (Cat#sc-2027; Santa Cruz Biotechnology) were used as controls. To analyze IGF1R and IR ubiquitination, cells were treated with 10 μM MG132 and/or 25 μM CQ for 24 h. The cells were lysed with RIPA buffer containing a protease inhibitor cocktail and centrifuged to obtain cytosolic proteins. Ubiquitinated IGF1R and IR were immunoprecipitated using IGF1R (Cat#ab39675; Abcam) or IR (Cat#3025S; Cell Signaling) antibodies, followed by immunoblotting with Ub antibody (Cat#sc-8017; Santa Cruz Biotechnology).

Immunofluorescence (IF). Cells were plated at a density of 5×10^4 cells in a confocal dish (Coverglass-Bottom Dish, Cat#100350; SPL) for 24 h. The cells were fixed in 4% paraformaldehyde for 15 min and washed three times with PBS. The cells were blocked with IF blocking buffer (PBS, 2% BSA, 0.3% Triton-X 100) for 1 h and stained with NEDD4-1 (Cat#sc-25508; Santa Cruz Biotechnology), IGF1R (Cat#sc-81464; Santa Cruz Biotechnology), and IR (Cat#3025S; Cell Signaling) in IF buffer for 12 h. Alexa Fluor® 568 (Cat#ab150115; Abcam) and Alexa Fluor® 647 (Cat#ab175473; Abcam) were diluted 1:100 in IF blocking buffer. The nuclei were stained with DAPI (Cat#P36931; Invitrogen) for 10 min after washing with PBS. Confocal images were obtained using a Zeiss confocal microscope (A1 confocal microscope; Nikon).

Immunohistochemical (IHC) analysis. The mouse organs were dissected and fixed in 4% formalin overnight at room temperature. The samples were washed with PBS and incubated in 70%, 80%, 95%, and 100% ethanol for 30 min each. They were then transferred to xylene for 4 h, embedded in paraffin, cut into 5-μm sections using a microtone, dried at room temperature, and deparaffinized at 60°C for 1 h. The slides were then incubated in 10 mM sodium citrate buffer (pH 6.0) at 100°C for 20 min, cooled, and then washed with distilled water for 5 min. Peroxidase activity was removed in methanol buffer containing 0.3% H_2O_2, washed three times with PBS for 5 min, and blocked with 5% BSA in PBS-T for 1 h at room temperature. The primary antibodies were diluted in blocking solution and used to incubate the sections overnight at 4°C. The following day, the slides were washed with PBS three times and incubated with a specific biotinylated secondary antibody at room temperature for 1 h. Color was developed using ABC KIT (Cat#pk-4000; VECTASTAIN®ABC). Finally, the slides were dehydrated and covered using a mounting medium.

Animal experiments. TRIP-Br1 knockout mice (RRID: MGI:4437096) with a C57BL/6 genetic background were kindly gifted by Dr. Huang (Hong Kong University of Science and Technology, Hong Kong, China). The mouse strains were genotyped using a PCR assay as described previously [40]. Insulin-deficient mice (C57BL/6-Tg(pH1-siRNAinsulin/CMV-hIDE)Korl) (5-week-old) were purchased from Laboratory Animal Resource Bank (https://lareb.nifds.go.kr/). Mouse embryo fibroblasts (MEF) were isolated as follows: the

embryos were dissected and decapitated from 13.5-day pregnant mice bearing wild-type or knockout TRIP-Br1, in which internal organs were removed. Then, the tissues were washed with cold PBS, cut into pieces, and incubated with trypsin/EDTA. Lastly, the cells were transferred to DMEM supplemented with 10% FBS after each incubation. These cells were maintained in DMEM after the removal of the non-adherent cells after 2 h.

Xenograft study. Exponentially growing $MCF7^{WT-TRIP-Br1}$ and $MCF7^{KD-TRIP-Br1}$ cells (1×10^7 cells) were collected and re-suspended in 0.1 ml of PBS. The cells were then subcutaneously injected into 5-week-old female null mice. The volumes of the resulting tumors were calculated as follows: $0.523 \times length \times width^2$. The mice were sacrificed after one month and their tumor weights were measured after resection.

Single-cell RNA sequencing analysis. Single-cell RNA-seq data for 11 breast cancer patients were downloaded from GEO (SRP066982). Sequencing reads from raw fastq were aligned using STAR v2.7.8a with the human reference genome GRCh38 and the Genecode.v38 annotations, and transcript per million (TPM) values were estimated using RSEM v1.3.1, with the following options: star–paired-end–estimate-rspd–single-cell-prior. The log2-tansformed TPM value, log2(TPM + 1), was considered as the relative expression level of each gene. Before further analysis, cells of reliable quality were collected after cell-type annotation, as defined in the original paper. To evaluate the association between two factors, we computed Pearson's correlation coefficient and performed linear regression analysis using the 'lm' function from the base package in R. The IR/IGF1R ratio was calculated by subtracting (or dividing) the relative expression of IR and IGF1R. Missing values due to a lack of IGF1R expression were removed from the association analysis.

Statistics analysis. Data are presented as the mean ± standard deviation (SD) from three independent experiments. Statistical analysis was performed using Student's t-test to compare two different groups or one-way analysis of variance followed by Bonferroni's multiple comparisons test to compare multiple groups. SPSS Statistics version 23 (IBM Corporation, Armonk, NY, USA) was used to analyze the data. $P < 0.05$ was used to denote statistical significance.

Results

The positive impact of TRIP-Br1 on IR expression results in a higher IR/IGF1R ratio

The effects of TRIP-Br1 expression on the IR/IGF1R ratio were initially evaluated in normal (MCF10A) and breast cancer cell lines (Fig. 1A-B). While normal cells showed similar IR and IGF1R expression levels, the majority of the breast cancer cell lines showed significantly higher levels of IR expression than IGF1R expression, resulting in a high IR/IGF1R ratio (Fig. 1A-B). In particular, four cancer cell lines (MDA-MB-453, MDA-MB-468, BT20, and BT549) with very high levels of TRIP-Br1 showed a much higher IR/IGF1R ratio than the other cancer cell lines (Fig. 1A-B). In our previous and unpublished studies, we found that TRIP-Br1 gene expression was always very high regardless of stressful stimuli in these four cell lines, while

TRIP-Br1 expression was greatly increased in MCF7 and MDA-MB-231 cell lines in response to various cell death-inducing stressful conditions [32]. Therefore, the MCF7 and MDA-MB-231 cell lines were selected for further study.

First, the impact of TRIP-Br1 on IR expression was tested in MEFs isolated from TRIP-Br1 wild-type ($MEF^{WT-TRIP-Br1)}$ and knockout ($MEF^{KO-TRIP-Br1)}$ mice. Interestingly, a higher level of IR expression was found in $MEF^{WT-TRIP-Br1}$ compared to $MEF^{KO-TRIP-Br1}$ cells (Fig. 1C-D). The knockout of TRIP-Br1 was confirmed by genotyping, as shown in **Supplementary Fig. S1A and S1B**. Similar results were obtained in the confocal immunofluorescence experiment (Fig. 1E-F). Furthermore, TRIP-Br1 wild-type mice also showed approximately 2–4 fold higher IR expression levels in adipocyte and heart tissue samples compared with TRIP-Br1 knockout mice (Fig. 1G-H). MCF7 cells with wild-type TRIP-Br1 ($MCF7^{WT-TRIP-Br1}$) also showed a much higher IR/IGF1R ratio than TRIP-Br1 knockdown stable MCF7 cells ($MCF7^{KD-TRIP-Br1}$) (Fig. 1I-J). $MCF7^{WT-TRIP-Br1}$ cells showed higher IR but lower IGF1R expression levels than MCF7KD-TRIP-Br1 cells (Fig. 1J-K). We also analyzed the total amount of IR and IGF1R using a co-antibody that recognizes both IGF1R and IR. No significant difference was detected between $MCF7^{WT-TRIP-Br1}$ and $MCF7^{KD-TRIP-Br1}$ cells, implying an inverse or compensatory relationship between them (Fig. 1J-K). Interestingly, we found an inverse relationship between IR and IGF1R expression. IR silencing significantly increased the IGF1R protein levels in MCF7 and MDA-MB-231 cells **(Supplementary S1C-D).** In a further study, much higher levels of IR ubiquitination were detected in $MCF7^{KD-TRIP-Br1}$ cells than in $MCF7^{WT-TRIP-Br1}$ cells after treatment with a proteasome inhibitor (MG132), but not with an autophagy inhibitor (CQ), suggesting that TRIP-Br1 suppresses proteasome-mediated degradation of IR (Fig. 1L-M).

These data clearly indicate that TRIP-Br1 positively regulates the expression of IR at the protein level, thereby enhancing the IR/IGF1R ratio.

Trip-br1-mediated Igf1r Downregulation Results In A Higher Ir/igf1r Ratio

TRIP-Br1 was found to contribute to a relatively high IR/IGF1R ratio by positively affecting IR expression. In addition, we examined the effects of TRIP-Br1 on IGF1R expression. First, the effect of TRIP-Br1 on IGF1R expression was tested in MCF7 and MDA-MB-231 cells. While TRIP-Br1 overexpression significantly decreased IGF1R expression (Fig. 2A-B), TRIP-Br1 silencing greatly increased IGF1R expression (Fig. 2C-D). In addition, $MCF7^{KD-TRIP-Br1}$ cells also showed much higher IGF1R expression than $MCF7^{WT-TRIP-Br1}$ cells (Fig. 2E-F). Furthermore, $MEF^{KO-TRIP-Br1}$ cells also showed a significant increase in IGF1R expression in comparison with $MEF^{WT-TRIP-Br1}$ (Fig. 2G-H). Lastly, TRIP-Br1 knockout mice showed elevated IGF1R in adipocytes (~ 20-fold) and the heart (~ 2-fold) compared to control mice (Fig. 2I-J).

Overall, these data strongly suggest that TRIP-Br1 negatively affects IGF1R expression, eventually increasing the IR/IGF1R ratio in breast cancer cells.

IGF1R protein levels decreased by TRIP-Br1 as an adopter protein and NEDD4-1 E3 ligase results in a higher IR/IGF1R ratio

Next, we investigated how TRIP-Br1 downregulates the IGF1R protein levels. TRIP-Br1 directly binds to two E3 ubiquitin ligases, NEDD4-1 and XIAP, as an adaptor protein [38–39, 41]. In addition, multiple lines of evidence have indicated that NEDD4-1 is an E3 ubiquitin ligase responsible for IGF1R degradation [42–46]. For example, oxidative stress-mediated NEDD4-1 upregulation degrades IGF1R during neurodegeneration [42]. However, no direct interaction between the IGF1R and NEDD4-1 has been reported, implying a possible constraint, such as the need for an adaptor protein. Therefore, we investigated whether TRIP-Br1 is responsible for the ubiquitination and degradation of IGF1R by interacting with NEDD4-1 or XIAP. Interestingly, the IGF1R expression levels were greatly increased in TRIP-Br1 and/or NEDD4-1 silenced MCF7 and MDA-MB-231 cell lines **(**Fig. 3A-B**)**. However, little change was observed in TRIP-Br1/XIAP double knockdown cells **(Supplementary Fig. S2**). The effect of NEDD4-1 on IGF1R degradation was also assessed. The IGF1R protein levels increased considerably after NEDD4-1 silencing in the presence of cycloheximide (CHX), a protein synthesis blocker (Fig. 3C-D). Co-immunoprecipitation experiments showed a direct interaction between TRIP-Br1 and IGF1R, as well as between NEDD4-1 (Fig. 3E-F). However, no direct interaction was observed between TRIP-Br1 and IR (Fig. 3E). Co-immunofluorescence experiments also revealed a higher co-localization of endogenous NEDD4-1 and IGF1R in $MCF7^{WT-TRIP-Br1}$ cells than in $MCF7^{KD-TRIP-Br1}$ cells, implying that TRIP-Br1 appears to serve as an adaptor protein to bring NEDD4 close enough to IGF1R (Fig. 3G-H).

Taken together, our data strongly suggest that TRIP-Br1 functions as an adapter protein and plays a vital role in NEDD4-1-mediated IGF1R downregulation.

Trip-br1/nedd4-1 Mediated Igf1r Degradation Through A Proteasome/ubiquitination

The degradation of many ligand-induced receptors is mediated through the ubiquitination of the receptors, followed by proteasome- or lysosome-dependent degradation. The binding of IGF1 to IGF1R leads to the polyubiquitination of IGF1R [47].Our previous and unpublished data showed that TRIP-Br1 plays an important role in both pathways [39, 41]. Thus, we evaluated which pathway is responsible for TRIP-Br1/NEDD4-1 mediated IGF1R degradation. To test this hypothesis, siNEDD4-1 was transfected into $MCF7^{WT-TRIP-Br1}$ and $MCF7^{KD-TRIP-Br1}$ cells in the absence or presence of MG132 or CQ. NEDD4-1 silencing significantly increased the IGF1R protein levels in the presence of MG132 **(**Fig. 4A-B**)** but only slightly increased after CQ treatment in $MCF7^{WT-TRIP-Br1}$ cells **(**Fig. 4C-D**)**. Similar results were obtained for the IGF1R expression levels after treatment with MG132 **(**Fig. 4E-F) but not with CQ (data not shown).

These findings suggest that TRIP-Br1/NEDD4-1-mediated IGF1R degradation occurs mainly through the proteasome/ubiquitination pathway rather than through a lysosomal pathway.

Enhanced Tumor Formation Is Associated With A Higher Ir/igf1r Ratio Resulting From Trip-br1 Expression

Next, we examined the IR/IGF1R ratio in TRIP-Br1-mediated tumor formation and growth using a xenograft model. $MCF7^{WT-TRIP-Br1}$ and $MCF7^{KD-TRIP-Br1}$ cells were subcutaneously injected into nude mice and tumor size was measured on the indicated days (Fig. 5A). Our results revealed a significant reduction in the tumor volume in $MCF7^{KD-TRIP-Br1}$ pretreated mice (Fig. 5A-B). A marked decrease (> 90%) in tumor weight was observed in tumors collected from null mice injected with $MCF7^{KD-TRIP-Br1}$ compared with $MCF7^{WT-TRIP-Br}$, suggesting that TRIP-Br1 is effective in strengthening *in vivo* tumor formation and growth (Fig. 5C). In agreement with the *in vitro* observations, an approximately 10-fold higher IR/IGF1R ratio, due to the higher IR but lower IGF1R, was detected in $MCF7^{WT-TRIP-Br1}$ cells grown in null mice. This suggests that a higher IR/IGF1R ratio could enhance the growth and proliferation of breast cancer cells (Fig. 5D-F). This result is consistent with those of previous studies. Although the inhibition of IGF1R was previously reported to not affect tumor growth in preclinical trials, it was found to enhance the IR signaling pathway, enhancing multistage tumors as a result [29–30]. These results suggest that IR, rather than IGF1R, may be responsible for the better growth and survival of cancer cells. This hypothesis was tested by examining the effect of IR on the survival of MCF7 cells in response to three different anticancer drugs (doxorubicin, staurosporine, and paclitaxel), namely, resistance to anticancer-mediated cell death. The MCF7 cell line is well known for its high resistance to programmed cell death against various anticancer drugs. Cell viability was found to be lower in IR-silenced MCF7 cells than in control cells after treatment with anticancer drugs (Fig. 5G**).**

Overall, these results indicate that TRIP-Br1 provides breast cancer cells with a better capacity for proliferation and survival by increasing the IR/IGF1R ratio even after treatment with anticancer drugs.

TRIP-Br1 induces a higher IR/IGF1R ratio in insulin-deficient mice mimicking diabetes

The effect of TRIP-Br1 on the IR/IGF1R ratio and the inverse relationship between IR and IGF1R expression were further tested in insulin-deficient mice mimicking diabetes patients, in which decreased insulin and increased glucagon levels were used as controls (Fig. 6A-B**)**. As in our previous studies, in which a deficiency of insulin or IGF1 was found to trigger TRIP-Br1 upregulation in breast cancer cells [32], a similar pattern was observed in our animal model (Fig. 6A-B**)**. Insulin-deficient mice showed significantly elevated TRIP-Br1 protein levels, which were accompanied by increased IR but decreased IGF1R in all three examined tissue samples (heart, liver, and adipocytes), confirming the positive effect of TRIP-Br1 on the higher IR/IGF1R ratio (Fig. 6A-B**)**. Representative images of immunohistochemical staining for TRIP-Br1, IR, and IGF1R in insulin-deficient mice and the corresponding normal mouse tissues are shown in Fig. 6C. Again, significantly higher TRIP-Br1 and IR, but lower IGF1R expression levels, were observed in insulin-deficient mice compared to normal mouse tissues, resulting in a higher IR/IGF1R ratio

in insulin-deficient mice (Fig. 6D). These findings strongly suggest that TRIP-Br1 positively regulates IR but negatively regulates IGF1R expression, resulting in a higher IR/IGF1R ratio, even in insulin-deficient mice.

Taken together, these results imply that TRIP-Br1 is also at least partly responsible for the induction of a higher IR/IGF1R ratio in patients with diabetes and breast cancer.

Discussion

To further elucidate the relationship between TRIP-Br1 expression and the IR/IGF1R ratio, we analyzed 317 tumor single cells from 11 breast cancer patients, as shown in GSE75688 datasets, which are divided into four representative subtypes **(Table 1)**. Unexpectedly, no significant relationship was found between TRIP-Br1 and IR expression in any of the four subtypes (Fig. 7A). However, triple-negative breast cancer (TNBC, $HR^-/HER2^-$) tumor cells showed a negative correlation between TRIP-Br1 and IGF1R expression (Fig. 7B). Accordingly, a positive correlation between the TRIP-Br1 expression levels and the IR/IGF1R ratio was found in TNBC (Fig. 7C). The TNBC subtype is known to induce the lowest survival rate in breast cancer patients compared to other subtypes. In addition, a study from the same GSE75688 datasets revealed that TNBC showed higher EMT and recurrence scores than luminal subtypes [50]. These results imply that TNBC with a TRIP-Br1-mediated higher IR/IGF1R ratio may lead to worse tumor progression and metastasis. The luminal A subtype (LumA, $HR^+/HER2^-$) showed the opposite results, in which only two patients were tested (Fig. 7A-C). However, our bioinformatics analysis (http://timer.cistrome.org/) from the database, with as many as 568 patients, showed an inverse relationship between TRIP-Br1 and IGF1R expression, similar to our *in vitro* results (Fig. 7D). Interestingly, an inverse relationship between IR and IGF1R expression was observed in these two subtypes.

In the present study, TRIP-Br1-mediated higher IR/IGF1R ratio was found to enable the proliferation and survival of breast cancer cells. In addition to our invaluable study on the importance of the IR/IGF1R ratio in breast cancer research, it would be very interesting to extend our research to other types of cancers. Therefore, we evaluated the effect of the TRIP-Br1-mediated IR/IGF1R ratio on the survival time of patients with other types of cancer, in addition to breast cancer patients, using the Cancer Genome Atlas (TCGA) database. Based on the mRNA levels of TRIP-Br1, IGF1R, and IR from TCGA database, we determined the survival time of three types of cancer patients at two different stages (stage i-ii and iii-x). Our bioinformatics analysis revealed that TRIP-Br1 was positively correlated with the IR/IGF1R ratio but inversely correlated with survival time in breast cancer patients (n = 152). However, no significant relationship was observed with lung (n = 396) or liver cancer (n = 130) (Fig. 8A-C). This implies that TRIP-Br1 may be a breast cancer-specific oncogenic adaptor protein. TRIP-Br1 may shorten the survival time of breast cancer patients by increasing the IR/IGF1R ratio, but not in lung and liver cancer patients. However, these results will need to be verified through accompanying *in vitro* and *in vivo* experiments.

It was proposed that NEDD4-1 can also be close to IGF1R through the growth factor receptor-bound protein 10 (Grb10) adapter protein [43]. Grb10 helps NEDD4-1 degrade IGF1R in mouse embryo fibroblast

p6 cells, as in the case of TRIP-Br1. We suspected that TRIP-Br1 may regulate NEDD4-1-mediated IGF1R degradation via Grb10 expression. However, our data revealed that Grb10 expression was much higher in $MCF7^{KD-TRIP-Br1}$ cells than in $MCF7^{WT-TRIP-Br1}$ cells **(Supplementary S3)**, implying that TRIP-Br1 negatively affected Grb10 expression. We suspected that NEDD4-1 may degrade IGF1R by changing the adapter protein under different environmental conditions or genetic backgrounds.

We showed that TRIP-Br1 suppressed ubiquitin/proteasome-mediated IR degradation, implying a negative effect of TRIP-Br1 on unknown E3 ligases that are responsible for the ubiquitination and degradation of IR, such as CHIP or MARCH1 [51–52]. Therefore, we hypothesized that TRIP-Br1 may inhibit the ubiquitination and degradation of IR by negatively affecting them.

We showed that IR negatively affected IGF1R expression. In contrast, we also attempted to elucidate the effect of the IGF1R on IR expression. Although the exact mechanism by which IGF1R regulates IR remains to be fully understood, it has been proposed that IGF1R downregulation does not directly affect IR expression, but rather increases sensitivity to insulin [48].

IR and IGF1R can activate the PI3K-AKT signaling pathway, which enhances the proliferation and survival of cancer cells. Our findings also indicated that the phosphorylation level of AKT on the Ser473 residue was markedly reduced when treated with OSI-906, a dual inhibitor of IGF1R and IR **(Supplementary S4. A-B)**, suggesting that IGF1R and IR positively regulate the AKT signaling pathway. Zhang *et al.* showed that the insulin-mediated phosphorylation of Akt was greatly enhanced when IGF1R was downregulated in breast cancer cells [48]. They proposed that the increase in insulin signaling upon IGF1R downregulation is a common phenomenon among breast cancer cells [48]. Taking our findings together, we propose the hypothesis that a higher IR/IGF1R ratio, with upregulated IR but downregulated IGF1R, may highly activate the PI3K-AKT signaling pathway, which subsequently enhances the proliferation and survival of cancer cells (Fig. 9).

In conclusion, our findings provide valuable information on the regulatory mechanisms of the IR/IGF1R ratio. In this study, we showed that a TRIP-Br1-mediated higher IR/IGF1R ratio increased the survival rate of breast cancer cells, resulting in a worse prognosis for cancer patients. Therefore, the TRIP-Br1-mediated IR/IGF1R ratio appears to be a predictive factor for the prognosis and progression of cancer.

Abbreviations

IR: insulin receptor; IGF1R: insulin-like growth factor-1 receptor; TRIP-Br1: transcriptional regulator interacting with the PHD-bromodomain 1; NEDD4-1: neural precursor cell expressed developmentally downregulated protein 4-1

Declarations

Ethical Approval and Consent to participate

This project was approved by Sookmyung Women's University Institutional Animal Care and Use Committee: SMU-IACUC (SMWU-IACUC-1701-043-03, SMWU-IACUC-1701-043-02,SMWU-IACUC-1701-043-01).

Consent for publication

Not applicable.

Availability of supporting data

All the data supporting the findings of this study are available within the article and its additional files and from the corresponding author upon reasonable request.

Competing interests

The authors declare that they have no competing interests.

Funding

This research was supported by the Basic Science Research Program through the National Research Foundation of Korea (NRF) funded bythe National Research Foundation of Korea (NRF-2016R1A5A1011974) and (NRF-2020R1A2C1102100).

Authors' contributions

NTNQ and SJ were responsible for designing, conducting the research, extracting and analyzing data, interpreting results, writing the manuscript. NHA and BL contributed in handling animal experiment. MRK contributed IHC protocol. HOL and HHE participated in the interpretation of single cell analysis. DJ, TJ, YC contributed in molecular experiment. MSL made substantial contribution to the conception of the study and the experimental design, revised the manuscript and gave the final approval for the publication of the manuscript.

Acknowledgements

We would like to thank Dr. Huang (Hong Kong University of Science and Technology, Hong Kong, China) for providing TRIP-Br1 knockout mice (RRID: MGI:4437096). We thank Editage (www.editage.co.kr) for English language editing.

References

1. Wang H, *et al.* Global, regional, and national life expectancy, all-cause mortality, and cause-specific mortality for 249 causes of death. The Lancet. 2016;388(10053):1459-1544.
2. Sung H, Ferlay J, Siegel RL, Laversanne M, Soerjomataram I, Jemal A, Bray F. Global cancer statistics 2020: GLOBOCAN estimates of incidence and mortality worldwide for 36 cancers in 185 countries.

CA Cancer J Clin. 2021;71:209-249.

3. Garg SK, Maurer H, Reed K, Selagamsetty R. Diabetes and cancer: two diseases with obesity as a common risk factor. Diabetes Obes Metab. 2014;16(2):97-110.
4. Giovannucci E, Harlan DM, Archer MC, Bergenstal RM, Gapstur SM, Habel LA, Pollak M, Regensteiner JG, Yee D. Diabetes and cancer: a consensus report. Diabetes Care, 2010; 33(7):1674-1685.
5. Maskarinec G, Jacobs S, Park SY, Haiman CA, Setiawan VW, Wilkens LR, Marchand LL.Type II Diabetes, Obesity, and Breast Cancer Risk: The Multiethnic Cohort. Cancer Epidemiol Biomarkers Prev. 2017;26(6):854-861.
6. Larsson SC, Mantzoros CS, Wolk A. Diabetes mellitus and risk of breast cancer: A meta-analysis. Int J Cancer, 2007;121:856–862.
7. Wolf I, Sadetzki S, Catane R, Karasik A, Kaufman B.Diabetes mellitus and breast cancer. Lanet Oncol. 2005;6(2):103-111.
8. Martin SD, and McGee SL.Metabolic reprogramming in type 2 diabetes and the development of breast cancer. J Endocrinol. 2018;237(2):35-46.
9. Bronsveld HK, Jensen V, Vahl P, De Bruin ML, Cornelissen S, Sanders J, Auvinen A, Haukka J, Andersen M, Vestergaard P, Schmidt MK.Diabetes and Breast Cancer Subtypes. PloS One. 2017; 12(1):e0170084.
10. Cai W, Sakaguchi M, Kleinridders A, Pino GGD, Dreyfuss JM, O'Neill BT, Ramirez AK, Pan H, Winnay JN, Boucher J, Eck MJ, Kahn CR.Domain-dependent effects of insulin and IGF-1 receptors on signalling and gene expression. Nat Commun. 2017;8:14892.
11. Ullrich A, Gray A, Tam AW, Yang-Feng T, Tsubokawa M, Collins C, Henzel W, T Le Bon T, S Kathuria S, Chen E.Insulin like growth factor I receptor primary structure comparison with insulin receptor suggests structural determinants that define functional specificity. The EMBO J. 1986;5(10):2503-2512.
12. Swinnen SG, Hoekstra JB, DeVries JH.Insulin therapy for type 2 diabetes. Diabetes Care. 2009;32(Suppl 2):S253-9.
13. Teppala S and Shankar A. Association between serum IGF-1 and diabetes among U.S. adults. Diabetes Care, 2010;33(10):2257-2259.
14. Cabail MZ, Li S, Lemmon E, Bowen M, SR, Miller WT.The insulin and IGF1 receptor kinase domains are functional dimers in the activated state. Nat Commun, 2015;6:6406.
15. Soos MA, Whittaker J, Lammers R, Ullrich RA, Siddle K.Receptors for insulin and insulin-like growth factor-I can form hybrid dimers. Characterisation of hybrid receptors in transfected cells. Biochem J. 1990;270(2):383–390.
16. Belfiore A, Frasca F, Pandini G, Sciacca L, Vigneri R.Insulin receptor isoforms and insulin receptor/insulin-like growth factor receptor hybrids in physiology and disease. Endocr Rev. 2009;30(6):586-623.

17. Boucher J, Kleinridders A, Kahn CR, Insulin receptor signaling in normal and insulin-resistant states. Cold Spring Harb Perspect Biol. 2014;6(1):a009191.
18. Murphy N, Knuppel A, Papadimitriou N, Martin RM, Tsilidis KK, Smith-Byrne K, Fensom G, Perez-Cornago A, Travis RC, Key TJ, Gunter MJ.Insulin-like growth factor-1, insulin-like growth factor-binding protein-3, and breast cancer risk: observational and Mendelian randomization analyses with approximately 430 000 women. Ann Oncol. 2020;31(5):641-649.
19. Eliassen AH, Tworoger SS, Mantzoros CS, MN, Hankinson SE.Circulating insulin and c-peptide levels and risk of breast cancer among predominately premenopausal women. Cancer Epidemiol Biomarkers Prev. 2007;16(1):161-164.
20. Girnita L, Takahashi SI, Crudden C, Fukushima T, Worrall C, Furuta H, Yoshihara H, Hakuno F, Girnita A.Chapter Seven - When Phosphorylation Encounters Ubiquitination: A Balanced Perspective on IGF-1R Signaling. Prog Mol Biol Transl Sci. 2016;141:277-311.
21. Brahmkhatri VP, Prasanna C, Atreya HS, Insulin-like growth factor system in cancer: novel targeted therapies. Biomed Res Int. 2015;2015:538019.
22. Ireland L, Santos A, Campbell F, Figueiredo C, Hammond D, Ellies LG, Weyer-Czernilofsky U, Bogenrieder T, Schmid M, Mielgo A.Blockade of insulin-like growth factors increases efficacy of paclitaxel in metastatic breast cancer. Oncogene. 2018;37(15):2022-2036.
23. Rostoker R, Abelson S, Bitton-Worms K,Genkin I, Ben-Shmuel S, Dakwar M, Orr ZS, Caspi A, Tzukerman M, LeRoith D.Highly specific role of the insulin receptor in breast cancer progression. Endocr Relat Cancer. 2015;22(2):145-157.
24. Pollak M.The insulin and insulin-like growth factor receptor family in neoplasia: an update. Nat Rev Cancer. 2012;12(3):159-169.
25. Hua H, Kong Q, Yin J, Jiang Y.Insulin-like growth factor receptor signaling in tumorigenesis and drug resistance: a challenge for cancer therapy. J Hematol Oncol.2020;13(1):64.
26. Malaguarnera R and Belfiore A, The Insulin Receptor: A New Target for Cancer Therapy. Front Endocrinol (Lausanne). 2011;2:93
27. Sun Y, Sun X, Shen B. Molecular Imaging of IGF-1R in Cancer. Mol Imaging., 2017;16:1536012117736648.
28. Pian L, Wen X, Kang L, Li Z, Nie Y, Du Z, Dehai Yu D, Lei Zhou L, Lin Jia L, Chen N, Li D, Zhang S, Li W, Hoffman AR, Sun J, Cui J, Hu JF. Targeting the IGF1R Pathway in Breast Cancer Using Antisense lncRNA-Mediated Promoter cis Competition. Mol Ther Nucleic Acids. 2018;12:105-117.
29. Buck E, Gokhale PC, Koujak S, Brown E, Eyzaguirre A, Tao N, Rosenfeld-Franklin M, Lerner L, Chiu MI, Wild R, Epstein D, Pachter JA, Miglarese MR.Compensatory insulin receptor (IR) activation on inhibition of insulin-like growth factor-1 receptor (IGF-1R): rationale for cotargeting IGF-1R and IR in cancer. Mol Cancer Ther. 2010;9(10):2652-64.
30. Ulanet DB, Ludwig DL, Kahn CR, Hanahan D. Insulin receptor functionally enhances multistage tumor progression and conveys intrinsic resistance to IGF-1R targeted therapy. PNAS. 2010;107(24):10791-10798.

31. Gallagher EJ, K, SM, E, Friedman NB, Boolbol SK, Killelea B, Pilewskie M, L, King T, Nayak A, Franco R, Cruz D, Antoniou IM, LeRoith D, NA.Insulin resistance contributes to racial disparities in breast cancer prognosis in US women. Breast Cancer Res. 2020;22(1):40.
32. Jung S, Li C, Duan J, Lee S, Kyeri Kim K, Park Y, Yang Y , Kim KI, Lim JS, Cheon CI, YS, Lee MS.TRIP-Br1 oncoprotein inhibits autophagy, apoptosis, and necroptosis under nutrient/serum-deprived condition. Oncotarget. 2015;6(30):29060-29075.
33. Hong SW, Kim CJ, Park WS, Shin JS, Lee SD, Ko SG, Jung S, Park IC, An SK, Lee WK, Lee WJ, Jin DH, Lee MS.p34SEI-1 inhibits apoptosis through the stabilization of the X-linked inhibitor of apoptosis protein: p34SEI-1 as a novel target for anti-breast cancer strategies. Cancer Res. 2009;69(3):741-746.
34. Hsu SI, Yang CM, Sim KG, Hentschel DM, O'Leary E, Bonventre JV.TRIP-Br: a novel family of PHD zinc finger- and bromodomain-interacting proteins that regulate the transcriptional activity of E2F-1/DP-1. EMBO J. 2001;20(9):2273-2285.
35. Hong SW, Shin JS, Lee YM, Kim DG, Lee SY, Yoon DH, Jung SY, Hwang JJ, Lee SJ, Cho DH, Hong YS, Kim TW, Jin DH, Lee WK.p34 (SEI-1) inhibits ROS-induced cell death through suppression of ASK1. Cancer Biol Ther. 2011;12(5):421-426.
36. Li J, Muscarella P, Joo SH, Knobloch TJ, Melvin WS, Weghorst CM, Tsai MD.Dissection of CDK4-binding and transactivation activities of p34(SEI-1) and comparison between functions of p34(SEI-1) and p16(INK4A). Biochemistry. 2015;44(40):13246-13256
37. Lai IL, Wang SY, Yao YL, Yang WM. Transcriptional and subcellular regulation of the TRIP-Br family. Gene. 2007;388(1-2):102-109.
38. Hu W, Yu X, Liu Z, Sun Y, Chen X, Yang X, Li X, Lam WK, Duan Y, Cao X, Steller H, Liu K, Huang P.The complex of TRIP-Br1 and XIAP ubiquitinates and degrades multiple adenylyl cyclase isoforms. Elife. 2017;6:e28021.
39. Jung S, Li C, Dongjun Jeong D, Lee S, Ohk J, Park M, Han S, Duan J, Kim C, Yang Y, Kim KI, Lim JS, Kang YS, Lee MS.Oncogenic function of p34SEI-1 via NEDD41mediated PTEN ubiquitination/degradation and activation of the PI3K/AKT pathway. Int J Oncol.2013; 43(5):1587-1595.
40. Pablo J Fernandez-Marcos 1, Cristina Pantoja, Agueda Gonzalez-Rodriguez, Nicholas Martin, Juana M Flores, Angela M Valverde, Eiji Hara, Manuel Serrano. Normal proliferation and tumorigenesis but impaired pancreatic function in mice lacking the cell cycle regulator sei1. PloS One. 2010;5(1):e8744.
41. Hong SW, Moon JH, Kim JS, Shin JS, Jung KA, Lee WK, Jeong SY, Hwang JJ, Lee SJ, Y-A Suh YA, I Kim I, K-Y Nam KY, S Han S, Kim JE, Kim KP, Hong YS, Lee JL, Lee WJ, E K Choi EK, Lee JS, Jin DH, Kim TW.p34 is a novel regulator of the oncogenic behavior of NEDD4-1 and PTEN. Cell Death Differ. 2014;21(1):146-160.
42. Kwak YD, Wang B, Jing Jing Li JJ, Ruishan Wang R, Deng Q, Diao S, Chen Y, Xu R, Masliah E, Xu H, JJ, Liao FF.Upregulation of the E3 ligase NEDD4-1 by oxidative stress degrades IGF-1 receptor protein in neurodegeneration. J Neurosci. 2012;32(32):10971-10981.

43. Monami G, Emiliozzi V, Morrione A.Grb10/Nedd4-mediated multiubiquitination of the insulin-like growth factor receptor regulates receptor internalization. J Cell Physiol. 2008;216(2):426-437.
44. Huang Q and Szebenyi DM.Structural basis for the interaction between the growth factor-binding protein GRB10 and the E3 ubiquitin ligase NEDD4. J Biol Chem. 2010:285(53):42130-9.
45. Zhang Y, Goodfellow R, Li Y, Shujie Yang S, Winters CJ, Kristina W Thiel KW, Leslie KK, Yang B.NEDD4 ubiquitin ligase is a putative oncogene in endometrial cancer that activates IGF-1R/PI3K/Akt signaling. Gynecol Oncol. 2015;139(1):127-133.
46. Yan C, Minmeng Zhao M, Li S, Tongjun Liu T, Xu C, Liu L, Geng T, Gong D.Increase of E3 ubiquitin ligase NEDD4 expression leads to degradation of its target proteins PTEN/IGF1R during the formation of goose fatty liver. J AniSci. 2020;98(9):skaa270.
47. Kavran JM, McCabe JM, Byrne PO, Connacher MK, Wang Z, r Ramek A, Sarabipour S, Shan Y, Shaw DE, Hristova K, Cole PA, Leahy DJ.How IGF-1 activates its receptor. Elife. 2014;3:e03772.
48. Zhang H, Pelzer AM, Kiang DT, Yee D.Down-regulation of Type I Insulin-like Growth Factor Receptor Increases Sensitivity of Breast Cancer Cells to Insulin. Cancer Res. 2007;67(1):391-397.
49. Mittal V.Epithelial Mesenchymal Transition in Tumor Metastasis. Annu Rev Pathol. 2018;13:395-412
50. Chung WS, Eum HH, Lee HO, Lee KM, Lee HB, Kim KT, Ryu HS, Kim SM, Lee JE, Park YH,Kan Z, Han W, Park WY.Single-cell RNA-seq enables comprehensive tumour and immune cell profiling in primary breast cancer. Nat Commun. 2017;8(1):15081.
51. Tawo R, Pokrzywa W, Kevei E, Akyuz ME, Balaji V, Adrian S, Höhfeld J, Hoppe T. The Ubiquitin Ligase CHIP Integrates Proteostasis and Aging by Regulation of Insulin Receptor Turnover. Cell. 2017;169(3):470-482.e13.
52. Nagarajan A, Petersen MC, Nasiri AR, Butrico G, Fung A, Ruan HB, Kursawe R, Caprio S, Thibodeau J, MC, Sun L, Gao G, Bhanot S, Jurczak MJ, Green MR, Shulman GI, Wajapeye N. MARCH1 regulates insulin sensitivity by controlling cell surface insulin receptor levels. Nat Comun. 2016;7:12639.

Figures

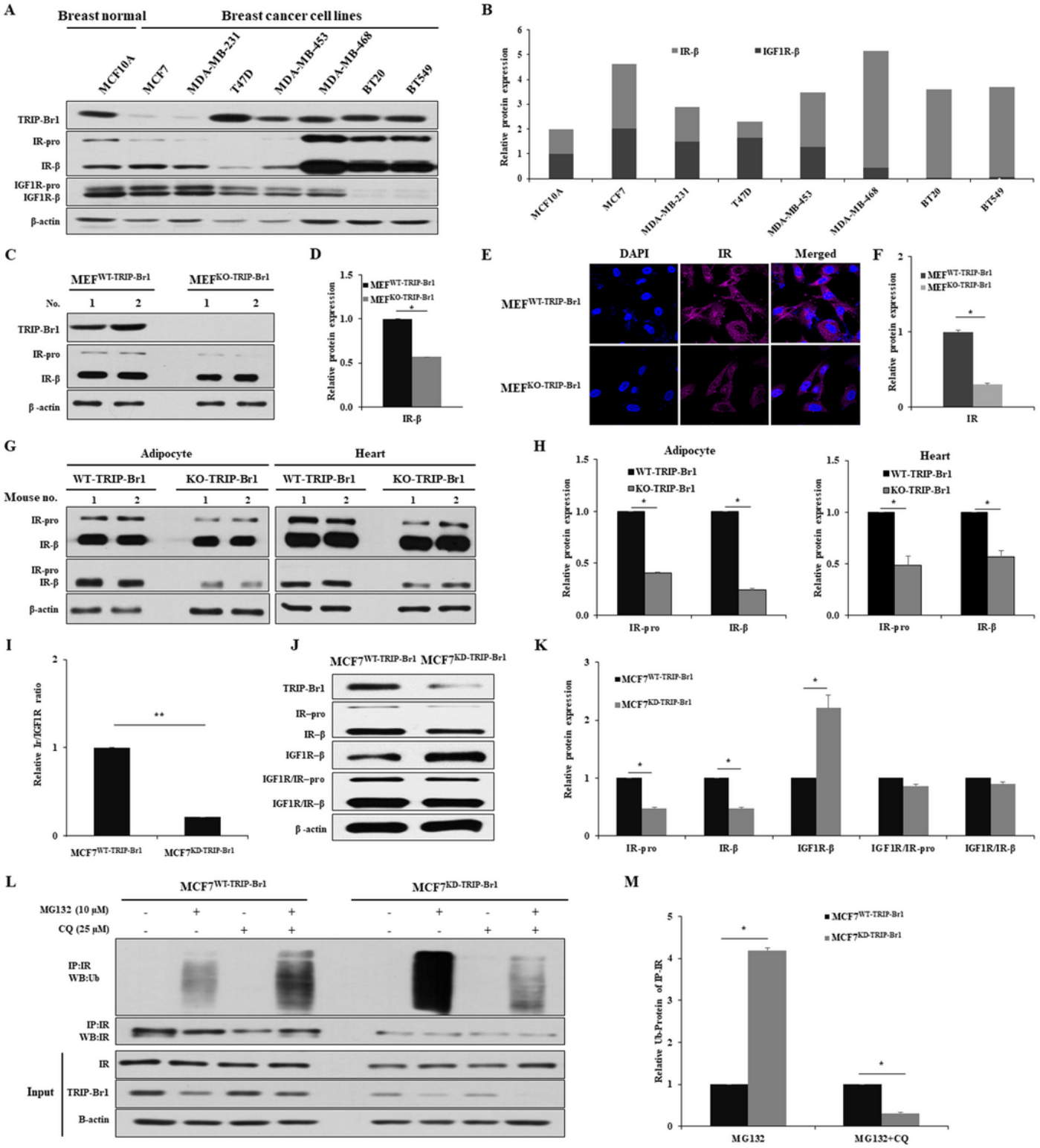

Figure 1

The IR/IGF1R ratio is increased by the positive impact of TRIP-Br1 on IR expression. A, Expression levels of TRIP-Br1, IGF1R, and IR in breast normal and cancer cell lines. β-actin was used as a loading control. **B,** IR/IGF1R ratio was quantified using ImageJ. **C-D,** Expression level of IR in MEF$^{WT\text{-}TRIP\text{-}Br1}$ or MEF$^{KO\text{-}TRIP\text{-}Br1}$ cells. Quantification of the western blots is shown as the mean ± SD based on three independent experiments (n = 3). Asterisk (*) indicates statistically significant difference at $p < 0.05$. **E-F,** Endogenous

IR expression was assessed in $MEF^{WT\text{-}TRIP\text{-}Br1}$ or $MEF^{KO\text{-}TRIP\text{-}Br1}$ cells by immunofluorescence (n > 30; *, p < 0.05). **G-H,** The IR protein levels from adipocytes and heart tissue collected from TRIP-Br1 wild-type or knockout mice were evaluated by western blotting (n = 3; *, p < 0.05). **I-J,**The relative IR/IGF1R ratio is shown in $MCF7^{WT\text{-}TRIP\text{-}Br1}$ and $MCF7^{KD\text{-}TRIP\text{-}Br1}$ cells.**J-K,**The indicated protein levels were evaluated in $MCF7^{WT\text{-}TRIP\text{-}Br1}$ and $MCF7^{KD\text{-}TRIP\text{-}Br1}$ cells. The expression of IGF1R and IR was co-analyzed using a co-antibody that recognizes both IGF1R and IR. Data are presented as the mean ± SD (n = 3; *, p < 0.05). **L,** $MCF7^{WT\text{-}TRIP\text{-}Br1}$ and $MCF7^{KD\text{-}TRIP\text{-}Br1}$ cells were treated with MG132 (10 μM) and/or CQ (25 μM) for 24 h. Endogenous IR was immunoprecipitated with anti-IR antibody. Ubiquitinated IR was analyzed with anti-Ub by employing western blot. **M,** Data are presented as the mean ± SD (n > 3; *, p < 0.05).

Figure 2

The IR/IGF1R ratio is enhanced via the TRIP-Br1-mediated downregulation of IGF1R. A-B, TRIP-Br1 was overexpressed by transfecting pcDNA3.1/TRIP-Br1 into MCF7 and MDA-MB-231 cells, in which pcDNA3.1 empty was used as a control. Cells were collected and prepared for western blot analysis. The results of western blotting were quantified using ImageJ. Analysis was conducted in triplicate and data are presented as the mean ± SD(n = 3; *, p < 0.05;**, p < 0.01). **C-D,** TRIP-Br1 silencing RNA (siTRIP-Br1) was transfected into MCF7 and MDA-MB-231 cells, in which scrambled RNA (scRNA) was used as a non-silencing control. Data are presented as the mean ± SD (n = 3; *, p < 0.05; **, p < 0.01; ***, p < 0.005). **E-F,** TRIP-Br1 and IGF1R expression levels in $MCF7^{WT\text{-}TRIP\text{-}Br1}$ and $MCF7^{KD\text{-}TRIP\text{-}Br1}$ cells.Data are presented as the mean ± SD (n = 3; *, p < 0.05;**, p < 0.01). **G-H,** TheTRIP-Br1 and IGF1R expression levels in $MEF^{WT\text{-}TRIP\text{-}Br1}$ or $MEF^{KO\text{-}TRIP\text{-}Br1}$ cells. MEF cells were isolated from TRIP-Br1 wild type or knockout mice, as mentioned in the Materials and Methods. Data are presented as the mean ± SD (n > 3; *, p < 0.05; ***, p < 0.005). **I-J,** The protein levels of TRIP-Br1 and IGF1R in adipocytes and heart tissue collected from TRIP-Br1 wild type or knockout mice. The results are presented as the mean ± SD (n = 3; *, p < 0.05; ***, p < 0.005).

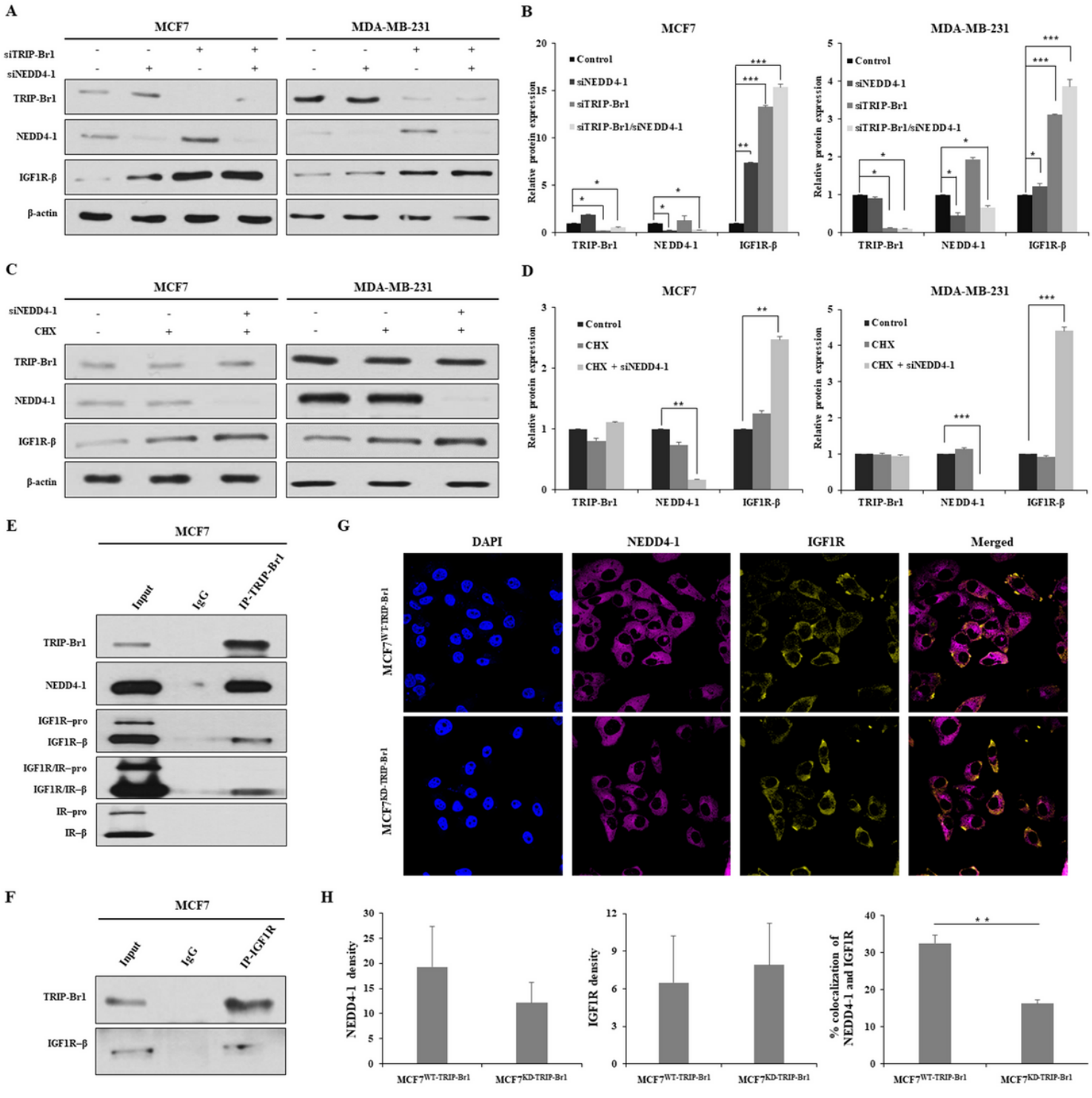

Figure 3

Decreased IGF1R protein level by TRIP-Br1 adopter protein and NEDD4-1 E3 ligase. A-B, TRIP-Br1 or NEDD4-1 silencing RNA (siTRIP-Br1 and siNEDD4-1) were transfected into MCF7 and MDA-MB-231 cells and IGF1R expression was analyzed by using a western blot analysis. Data are presented as the mean ± SD (n > 3; *, p < 0.05; **, p < 0.01; ***, p < 0.005). **C-D,** NEDD4-1 was knocked down by siNEDD4-1 in the presence of 200 mM CHX and the indicated proteins were subjected to western blot analysis. Data are presented as the mean ± SD (n > 3; *, p < 0.05; **, p < 0.01; ***, p < 0.005). **E-F,** The interaction between

IGF1R and TRIP-Br1 was determined by using co-immunoprecipitation assay. Endogenous TRIP-Br1 in MCF7 cells was immunoprecipitated with corresponding antibodies.**G-H,** The representative images of NEDD4-1 and IGF1R expression observed using a confocal microscope are shown. MCF7$^{WT\text{-}TRIP\text{-}Br1}$ and MCF7$^{KD\text{-}TRIP\text{-}Br1}$ cells were cultured in a confocal dish for 24 h and their immunofluorescence was analyzed. The co-localization between NEDD4-1 and IGF1R was measured by counting over 50 cells in ImageJ. Data are presented as the mean ± SD (n > 50, **, p < 0.01).

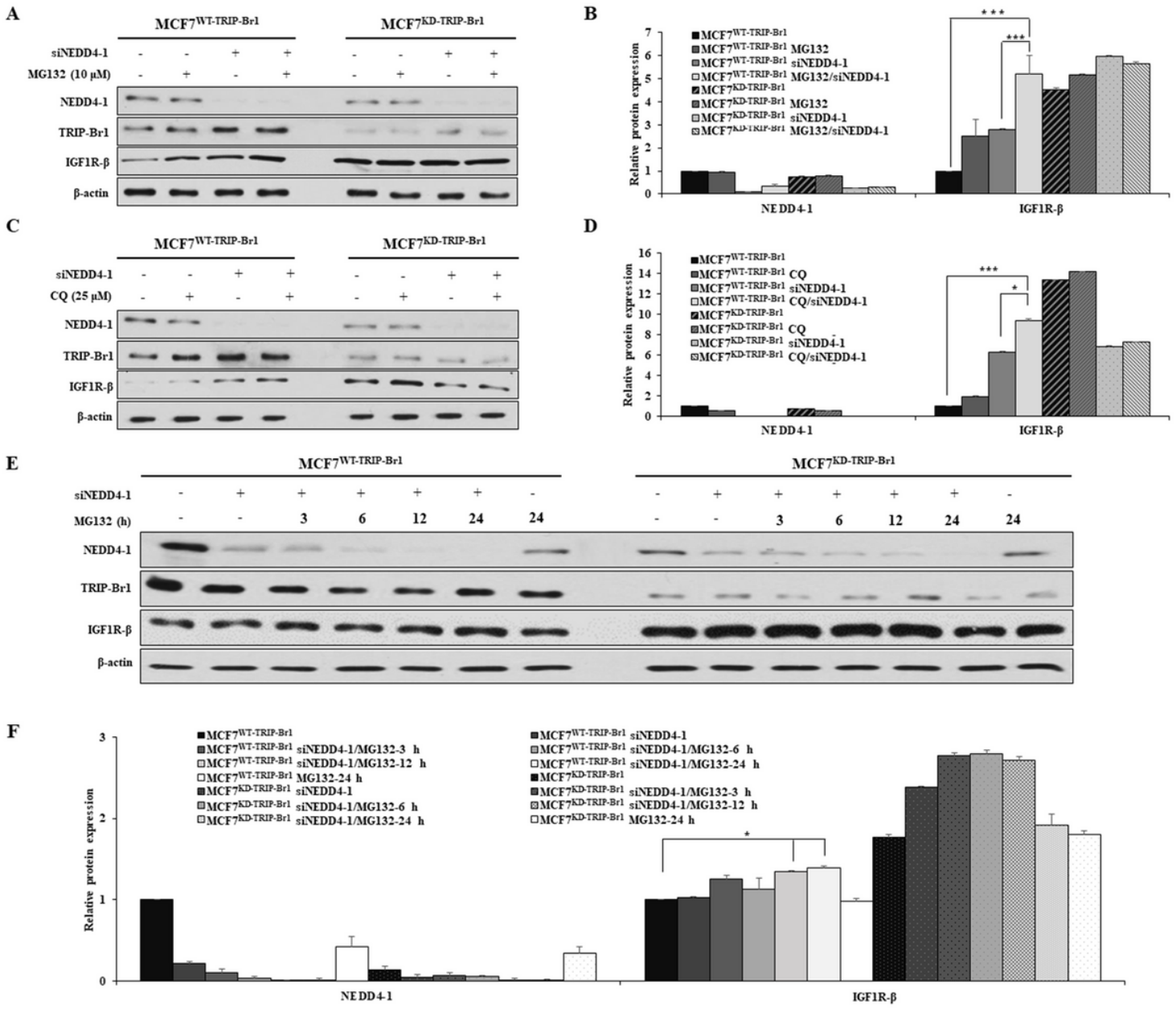

Figure 4

TRIP-Br1/NEDD4-1 mediates IGF1R degradation via a proteasome/ubiquitination and lysosome-dependent pathway. A-B, MCF7$^{WT\text{-}TRIP\text{-}Br1}$ and MCF7$^{KD\text{-}TRIP\text{-}Br1}$ cells were transfected with siNEDD4-1 in the

absence or presence of MG132 (10 μM) for 24 h. The cells were collected and subjected to western blotting. The quantification results are presented as the mean ± SD (n = 3; *, p < 0.05; **, p < 0.01; ***, p < 0.005). **C-D,** MCF7$^{WT\text{-}TRIP\text{-}Br1}$ and MCF7$^{KD\text{-}TRIP\text{-}Br1}$ cells were transfected with siNEDD4-1 with or without CQ (25 μM) for 24 h. Total cells were used to lysate and perform western blot analysis. Data are presented as mean ± SD (n = 3; *, p < 0.05; **, p < 0.01; ***, p < 0.005). **E-F,** MCF7$^{WT\text{-}TRIP\text{-}Br1}$ and MCF7$^{KD\text{-}TRIP\text{-}Br1}$ cells were transfected with siNEDD4-1 and treated with MG132 (10 μM) for the indicated times, and the cells were collected for the western blot analysis. The quantification of the western blots is shown as the mean ± SD (n = 3; *; p < 0.05).

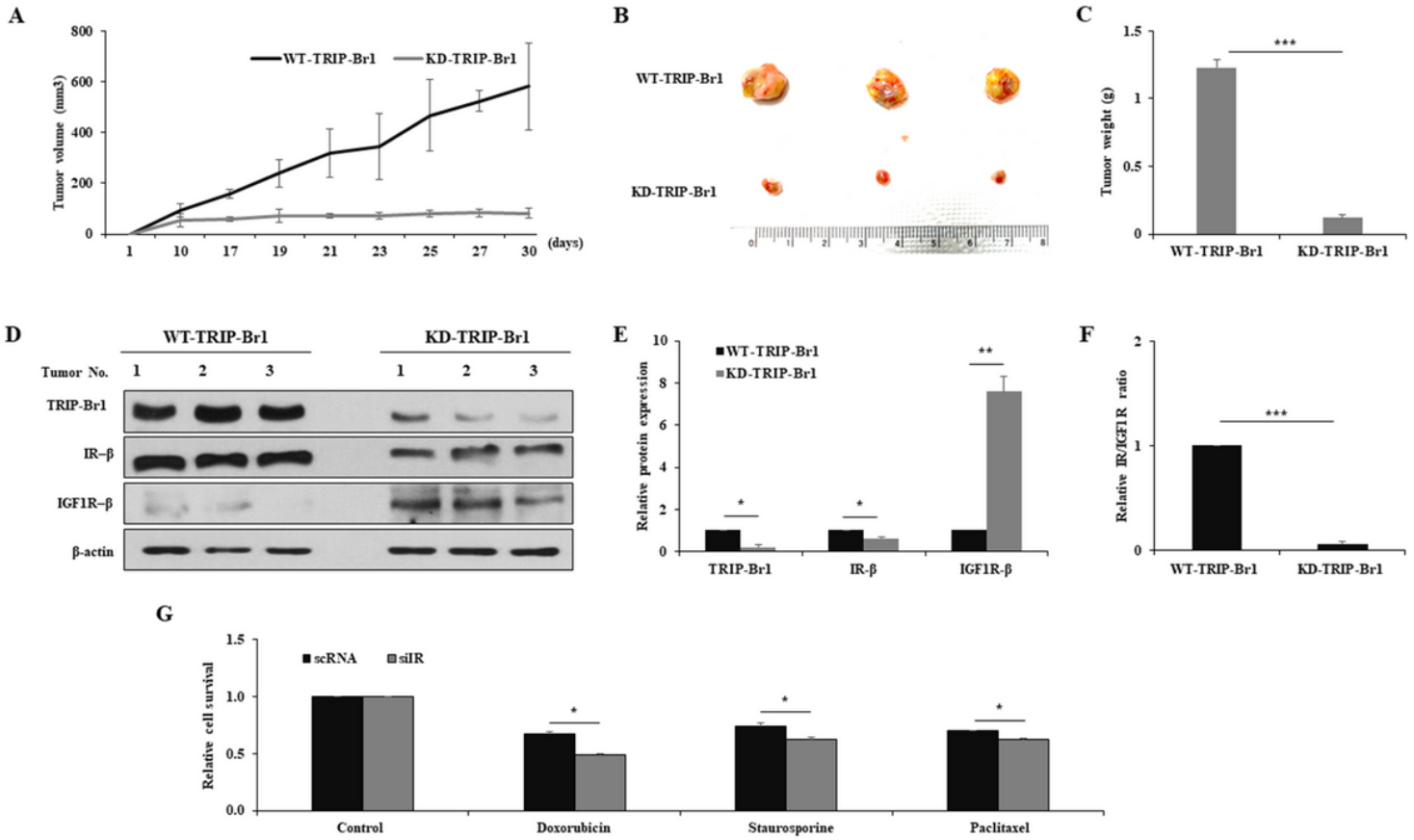

Figure 5

Enhanced tumor formation and growth is associated with a higher IR/IGF1R ratio resulting from TRIP-Br1 expression. A, Nude mice were subcutaneously injected in the flanks with MCF7$^{WT\text{-}TRIP\text{-}Br1}$ and MCF7$^{KD\text{-}TRIP\text{-}Br1}$ cells. The tumor volume was measured at the indicated times and calculated as described in Materials and Methods. **B,** Tumors were collected from null mice and photographed. Scale bar, 1 cm. **C,** Tumor weight was measured after mice resection. Data are presented as the mean ± SD (n = 4; ***, p < 0.005). **D-E,** The quantification of results are represented as the mean ± SD. (n = 4; *, p < 0.05; **, p < 0.01). **F,** The relative IR/IGF1R ratio is presented as the mean ± SD (n = 4, ***, p < 0.005). **G,** MCF7 cells were transfected with IR silencing RNAfor 24 h, seeded in 96-well plates, and treated with three different

types of anticancer drugs, doxorubicin (1 μM), stauroseporine (0.1 μM) and paclitaxel (0.5 μM) for 24 h. The cell viability was measured as mentioned in the Materials and Methods section. Data are presented as the mean ± SD (n = 3; *, p < 0.05).

Figure 6

The IR/IGF1R ratio is increased by TRIP-Br1 in insulin-deficient mice. A, Tissue samples from the heart, liver, and adipocytes were collected from 5-week-old insulin-producing mice (control) or insulin-deficient mice (IDM). The tissues were used to assess the levels of TRIP-Br1, IR, and IGF1R IR by western blot analysis, in which insulin and glucagon were used as controls. **B,** The quantification of results are presented as the mean ± SD (n > 3; *, p < 0.05; **, p < 0.01; ***, p < 0.005). The relative IR/IGF1R ratio is also shown. **C,** Representative images of IHC analysis showing the expression levels of TRIP-Br1, IR, and IGF1Rin the heart, liver and adipocytes of control or IDM groups. **D,** The expression levels of TRIP-Br1, IR, and IGF1Rare presented as the mean ± SD (n > 3; *, p < 0.05; ***, p < 0.005). The relative IR/IGF1R ratio is also shown.

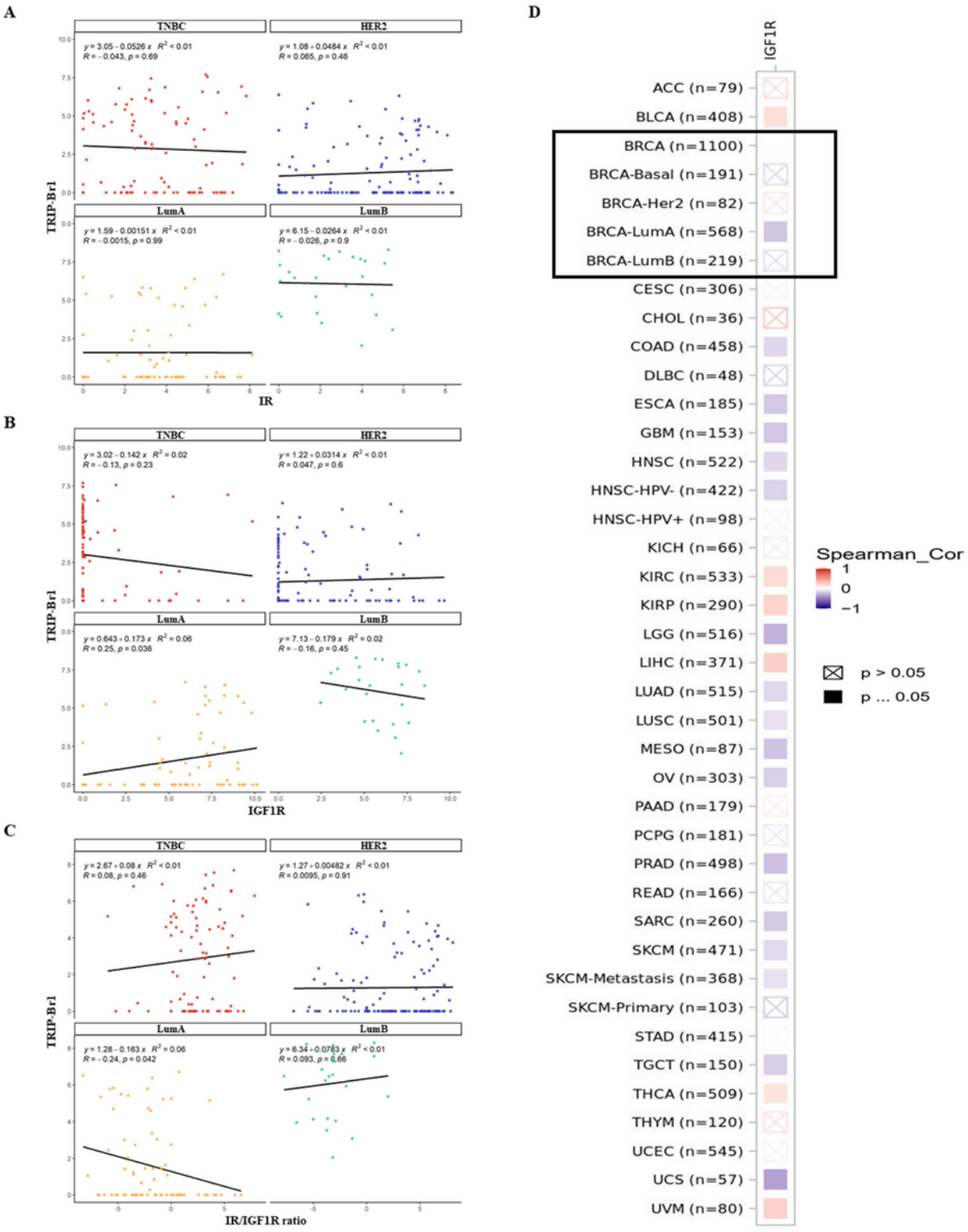

Figure 7

Correlation **between TRIP-Br1 and IR/IGF1R ratio in single cells from breast cancer patients. A,** The relationship of TRIP-Br1 and IRexpression in four different subtypes of breast cancer: TNBC, HER2, LumA, and LumB.**B,** The relationship of TRIP-Br1 and IGF1R expression in four different subtypes of breast cancer: **C,** The correlation of TRIP-Br1 and IR/IGF1R ratio in four subtypes of breast cancer. Each dot

represents a single cell.**D,** Analysis of the relationship of TRIP-Br1 and IGF1R expression by using timer2.0 tool (http://timer.cistrome.org/).

Figure 8

Bioinformatic analysis of the relationship between TRIP-Br1 expression, IR/IGF1R ratio, and the survival ratio in three differenttypes of cancer patients. The relationship between survival days and TRIP-Br1 expression or the IR/IGF1R ratio was analyzed in two groups (stage i-ii and stage iii-v) of indicated cancer patients using the TCGA database.

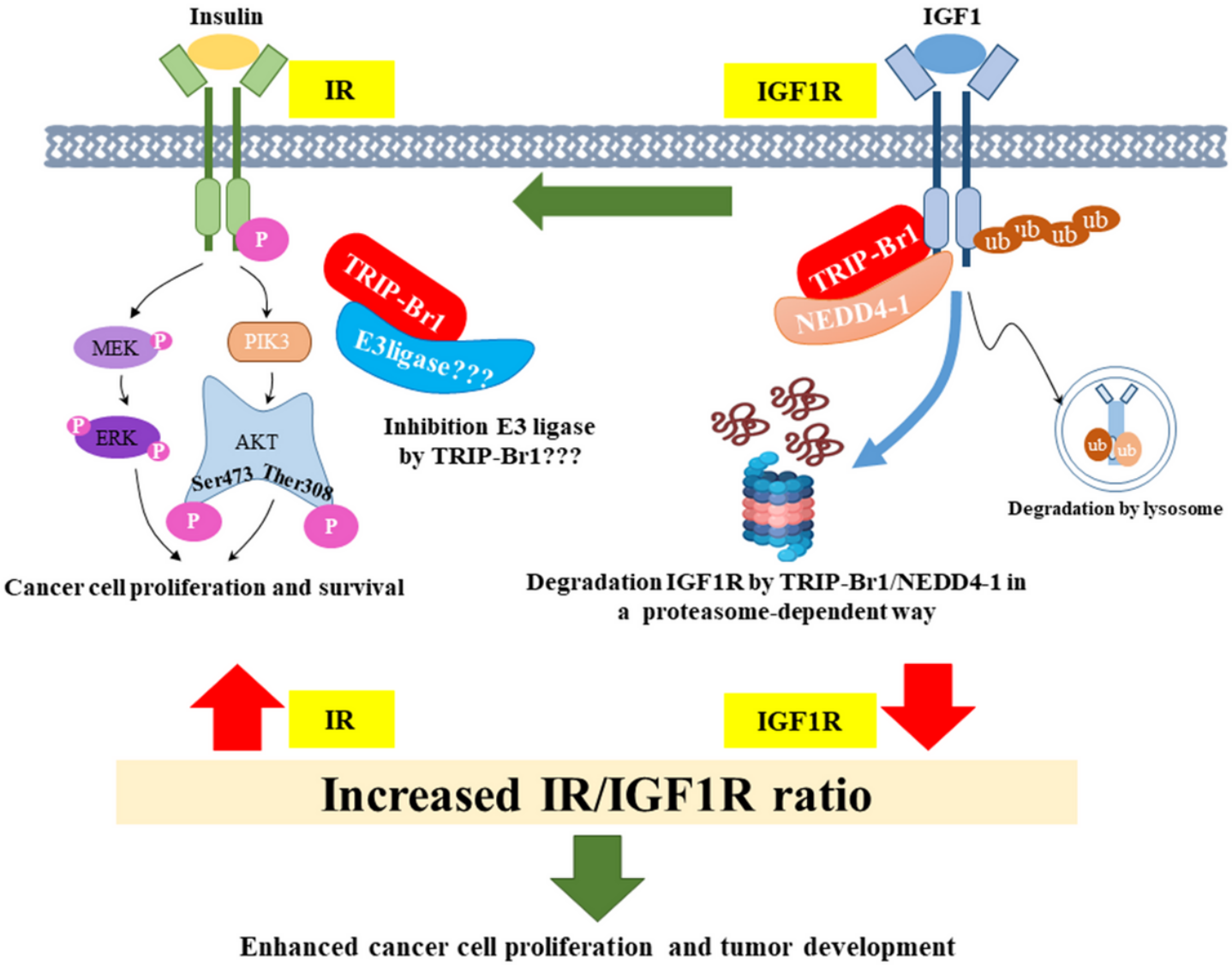

Figure 9

Summary model. The regulation of the IR/IGF1R ratio by TRIP-Br1 in breast cancer cells. TRIP-Br1 does not directly interact with IR and suppresses the proteasome-mediated degradation ubiquitination and degradation of IR, implying the negative effect on unknown E3 ligase, most likely CHIP or MARCH1. By contrast, TRIP-Br1 directly interacts with both IGF1R and NEDD4-1 E3 ubiquitin ligase, in which TRIP-Br1/NEDD4-1 degrades IGF1R via the ubiquitin/proteasome system rather than the lysosomal pathway. Eventually TRIP-Br1 increased the IR/IGF1R ratio and most likely worsened the prognosis of breast cancer patients. In addition, downregulated IGF1R is known to induce the IR activation, which eventually activates the PI3K/AKT and MAPK signaling pathways, resulting in the cancer cell proliferation and survival.

Supplementary Files

This is a list of supplementary files associated with this preprint. Click to download.

- SupplementaryS1.tif
- SupplementaryS2.tif
- SupplementaryS3.tif
- SupplementaryS4.tif
- SupplementaryTable1.tif